

Soft Matter

Accepted Manuscript



This is an *Accepted Manuscript*, which has been through the Royal Society of Chemistry peer review process and has been accepted for publication.

Accepted Manuscripts are published online shortly after acceptance, before technical editing, formatting and proof reading. Using this free service, authors can make their results available to the community, in citable form, before we publish the edited article. We will replace this *Accepted Manuscript* with the edited and formatted *Advance Article* as soon as it is available.

You can find more information about *Accepted Manuscripts* in the [Information for Authors](#).

Please note that technical editing may introduce minor changes to the text and/or graphics, which may alter content. The journal's standard [Terms & Conditions](#) and the [Ethical guidelines](#) still apply. In no event shall the Royal Society of Chemistry be held responsible for any errors or omissions in this *Accepted Manuscript* or any consequences arising from the use of any information it contains.

Invertible vesicles and micelles formed by dually-responsive diblock random copolymers in aqueous solutions†

*Mohammad T. Savoji, Satu Strandman, X.X. Zhu**

Department of Chemistry, Université de Montréal,

CP 6128, Succursale Centre-ville, Montreal, QC, H3C 3J7, Canada

Abstract

Dually-responsive diblock random copolymers poly(nPA_{0.8-co}-DEAEMA_{0.2})-block-poly(nPA_{0.8-co}-EA_{0.2}) were made from *N*-n-propylacrylamide (nPA), 2-(diethylamino)ethyl methacrylate (DEAEMA) and *N*-ethylacrylamide (EA) via reversible addition-fragmentation chain transfer (RAFT) polymerization. Copolymers of different block length ratios, poly(nPA_{28-co}-DEAEMA₇)-block-poly(nPA_{29-co}-EA₇) (P1) and poly(nPA_{28-co}-DEAEMA₇)-block-poly(nPA_{70-co}-EA₁₈) (P2), self-assemble into vesicles and micelles, responding to external stimuli in aqueous solutions, and both show “schizophrenic” inversion behavior when the pH and temperature are varied. The relative lengths of the two blocks are shown to affect the self-assembly of amphiphilic diblock copolymers. P1 has a similar length for both blocks and forms spherical vesicles with the first block poly(nPA_{29-co}-EA₇) as the membrane inner layer at pH 7 and 37 °C (above the cloud point of the more hydrophobic block, CP1), while spherical micelle-like aggregates are obtained at pH 10 and 25 °C (above CP1) with the second block poly(nPA_{28-co}-DEAEMA₇) as the core. In comparison, P2 has a different block length ratio (1:3, thus a much longer second block) and forms spherical micelles above CP1 at both pH 7 (the second block as the core) and pH 10 (the first block as the core). Further aggregation was observed by heating the polymer solution above the cloud point of the more hydrophilic block (CP2). The variation of the length and chemical composition of the blocks allows the tuning of the responsiveness of the block copolymers toward both pH and temperature and determines the formation of either micelles or vesicles during the aggregation.

Introduction

Amphiphilic block copolymers have attracted much research interest because of their capability of forming various self-assembled structures, particularly in aqueous solutions. Several reviews have been published on such amphiphilic systems and their self-assemblies.¹⁻⁸ The spontaneous self-assembly is the result of a balance between attractive and repulsive forces, such as hydrophobic interaction, hydrogen bonding, coordination to metals, and steric or electrostatic repulsion.⁹ Some parameters affecting this balance include the block ratio and the selectivity of the solvent. By introducing blocks responsive to different external stimuli, such as pH or temperature, it is possible to make systems that exhibit so-called “schizophrenic” behavior, forming invertible structures in aqueous solutions without the addition of organic solvents.¹⁰⁻¹³ The diblock copolymer based on 2-(*N*-morpholino)ethyl methacrylate (MEMA) and 2-(diethylamino)ethyl methacrylate (DEAEMA) was the first reported copolymer capable of switching between micelles and inverted micelles by the change in ionic strength or pH of the solution.¹⁰

The relative length of hydrophobic and hydrophilic segments is also expected to affect the self-assembly behavior of stimuli-responsive systems. We have earlier described the effect of adjusting the length of a single block on the aggregation mechanism of a thermo-responsive triblock terpolymer poly(*N*-*n*-propylacrylamide)-*block*-poly(*N*-isopropylacrylamide)-*block*-poly(*N,N*-ethylmethylacrylamide) (PnPA-*b*-PiPA-*b*-PEMA) in aqueous solutions.¹⁴ Homopolymers have been used as the consisting blocks in most reported block copolymers to obtain spherical micelles,¹⁵⁻¹⁷ disc-¹⁸⁻²⁰ and stacked disc-like micelles,¹⁹ rods,²¹ and various types of vesicles^{16, 22-25} in solution. More recently, thermoresponsive diblock copolymers consisting of random copolymers have been reported,^{26, 27} which self-assemble in aqueous solution at desired temperatures. The transition temperatures of individual blocks can be varied by adjusting their monomer compositions. In our previous work, we used this approach to prepare a symmetrical diblock random copolymer with tunable pH- and thermo-responsiveness, capable of forming invertible structures responding to changing stimuli.²⁸ This polymer was composed of two random copolymer blocks, one block responsive to temperature, poly(*N*-*n*-propylacrylamide-*co*-*N*-ethylacrylamide) (poly(nPA_{0.8-co}-EA_{0.2})), and the other responsive to both pH and temperature changes, poly[*N*-*n*-propylacrylamide-*co*-2-(diethylamino)ethyl methacrylate] (poly(nPA_{0.8-co}-DEAEMA_{0.2})). The pH-sensitive block became positively-charged below its pK_a

and thus more hydrophilic with a lower cloud point. As a result, switchable vesicles were obtained where the membrane inner and outer layers were inverted by changing the pH or the temperature. Due to the complexity of the obtained invertible systems, the aggregation mechanism of such diblock random copolymers remains to be better understood, especially the effect of the relative lengths of hydrophilic and hydrophobic segments on the aggregate morphology and the inversion process. In this work, we address this issue by changing the ratio of block lengths while keeping the block composition constant to explore the possibility of tuning the self-assembly behavior of dually stimuli-responsive diblock random copolymers, since the stimuli-induced inversion of the aggregates may be interesting for controlled loading and release applications.²⁹

Experimental

Materials. 2,2'-Azobisisobutyronitrile (AIBN, from Eastman Kodak) was recrystallized from methanol. Acryloyl chloride, ethylamine (70 % aqueous solution) and n-propylamine were purchased from Aldrich, and were used without further purification. 2-(Diethylamino)ethyl methacrylate (DEAEMA, from Aldrich) was vacuum-distilled prior to use. Previously reported procedures were followed in the preparation of the monomers N-n-propylacrylamide (nPA) and N-ethylacrylamide (EA)³⁰ and the chain transfer agent (CTA)3-(benzylsulfanylthiocarbonylsulfanyl)propionic acid (BPA).³¹ Anhydrous and oxygen-free tetrahydrofuran (THF) was obtained by passing the solvent through columns packed with activated alumina and supported copper catalyst (Glass Contour, Irvine, CA). Water was purified using a Millipore Milli-Q system.

Polymer synthesis. A previously reported method²⁸ was used to prepare diblock random copolymers with the same monomer ratios but different chain lengths. The first block, poly(nPA_{28-co}-DEAEMA₇), with a molar ratio of nPA:DEAEMA = 4:1 was synthesized with a molar ratio of 200:1:0.1 for the reaction mixture of [monomer]:[BPA]:[AIBN] during 60 min reaction time. The resulting random copolymer poly(nPA_{0.8-co}-DEAEMA_{0.2})-CTA was then chain-extended by RAFT copolymerization to provide another block with the same composition nPA : EA = 8:2 but different chain lengths. The first (P1) has nearly the same block length, poly(nPA_{28-co}-DEAEMA₇)-*block*-poly(nPA_{29-co}-EA₇), obtained from a reaction mixture of

[monomer]:[macro-CTA]:[AIBN] with molar ratio of 200:1:0.1 during 90 min, and the second (P2) has a longer second block, poly(nPA_{28-co}-DEAEMA₇)-*block*-poly(nPA_{70-co}-EA₁₈), with a reactant molar ratio [monomer]:[macro-CTA]:[AIBN] of 400:1:0.1 after 4 h.

Polymer characterization. Molar masses and polydispersity indices (PDI) of the polymers were determined by size exclusion chromatography (SEC) on a Waters 1525 system working with two Waters Styragel columns and a refractive index detector (Waters 2410). N,N-dimethylformamide (DMF) containing 0.01 M LiBr was used as the mobile phase at 50 °C with a flow rate of 1 mL/min. Poly(methyl methacrylate) standards were used for the molar mass calibration. The NMR spectra of the polymers were recorded on a Bruker AV-400 NMR spectrometer operating at 400 MHz for protons in deuterated chloroform (CDCl₃).

The formation of the polymer aggregates was studied by dynamic light scattering (DLS) conducted on a Malvern Zetasizer instrument (Nano ZS) equipped with a 4 mW He-Ne 633 nm laser. All solutions were prepared at a concentration of 0.05 mg/mL in pure Milli-Q water and dust was removed by filtering through 0.22- μ m Millipore filters. Measurements were conducted in a backscattering (173°) mode. Intensity-weighted hydrodynamic diameter (D_h) values were obtained as a function of temperature with a heating rate of ca. 0.1 °C/min.

The cloud points (CPs) of the polymers in aqueous solutions were determined from optical transmittance measured on a Cary 300 Bio UV-vis spectrophotometer with a Cary temperature controller in the wavelength range of 260-500 nm. Polymer solutions in deionized water (0.05 mg/mL) were continuously heated at a rate of 0.3 °C/min over different temperature ranges. The cloud point (CP) was taken as the middle point between the onset and the offset of abrupt change in the transmittance curve as a function of temperature.

Transmission electron microscopy (TEM) was performed on a FEI Tecnai 12 TEM at 120 kV, equipped with AMT XR80C CCD camera system. Aqueous solutions of the copolymers (0.05 mg/mL) were heated with a Cary temperature controller. The solution was deposited on copper grids (300 mesh, Carbon Type-B, Ted Pella, Inc.) at a desired temperature and rapidly frozen in liquid nitrogen. The samples were lyophilized and kept under vacuum until use.

Atomic force microscopy (AFM) images were acquired in air at room temperature using tapping mode at a scan rate of 1 Hz (Digital Instruments Dimension 3100 microscope, Santa

Barbara, CA). All images were acquired with a medium tip oscillation damping (20–30%). The samples were analyzed in the dried state via drop deposition of the 0.05 mg/mL aqueous solution of the polymer onto a mica surface at a desired temperature followed by lyophilization.

Results and discussion

Preparation of diblock random copolymers. The SEC chromatograms of the macro-CTA of the first block and the two final block copolymers are shown in Fig. 1, demonstrating the livingness of the block copolymerization. The conversions of the polymerizations were kept low (25%) to avoid the presence of dead chains, assuring the living character of macro-CTA and relatively low polydispersity of final block copolymers. The monomer compositions of mono- and diblock copolymers were calculated from ^1H NMR results, as described earlier.²⁸ The final compositions of the blocks were close to the initial monomer ratio in the feed, and the statistical nature of the macro-CTA random copolymer composed of acrylamide (nPA) and methacrylate (DEAEMA) monomers, despite their different reactivities, was assumed on the basis of frequent sampling of the reaction mixture and high reproducibility of the polymerization,²⁸ even though the possible formation of comonomer gradient^{32, 33} cannot be ruled out. The results of the block copolymerizations are summarized in **Table 1**.

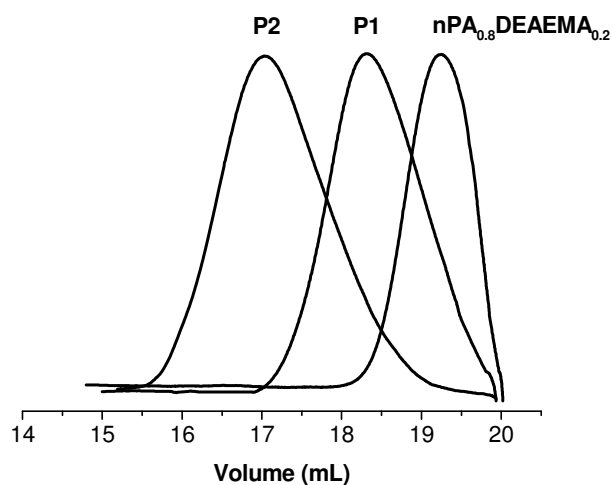


Fig. 1. SEC chromatograms of $\text{P}(\text{nPA}_{0.8}\text{DEAEMA}_{0.2})$ (macro-CTA), P1 and P2 in DMF. Solvent signals appearing at elution volume ~ 20 mL are excluded.

Table 1. Structural properties of mono- and diblock random copolymers.

Entry	P(nPA _{0.8-co} -DEAEMA _{0.2})		P(nPA _{0.8-co} -DEAEMA _{0.2})- <i>b</i> - P(nPA _{0.8-co} -EA _{0.2})			
	M _n , 1 st block ^a	PDI ^a	M _n , 2 nd block ^b	M _n , total ^a	PDI ^a	L (nm) ^c
P1	4,800	1.15	4,000	8,800	1.21	13.3
P2	4,800	1.15	12,100	16,900	1.30	20.4

^aDetermined by SEC in DMF against poly(methyl methacrylate) standards. ^bCalculated from SEC results. ^cContour length (L): the theoretical maximum length of the extended block copolymer polymer chain.

Thermo-responsiveness in aqueous solutions. We have previously shown that the thermo- and pH-responsiveness of the blocks can be adjusted according to their composition.^{26, 28} It was shown that the CPs of P(nPA_{0.8-co}-DEAEMA_{0.2}) copolymer at pH 7 and 10 are 52 and 13 °C, respectively,²⁸ although the CP slightly changes after addition of the second block. The pH-independent CP of P(nPA_{0.8-co}-EA_{0.2}) was found to be 33 °C.²⁶ In general, a higher fraction of the more hydrophobic comonomer (nPA) leads to a lower cloud point, while the protonation of DEAEMA moieties upon decreasing pH makes the dually stimuli-responsive block more hydrophilic, thus raising its cloud point. The relative block length is known to influence the morphologies of self-assembled structures, and the phase transition temperatures of the individual blocks in a dually-responsive block copolymer are interdependent.^{16, 22, 26, 28} In this work, the length of the dually responsive P(nPA_{0.8-co}-DEAEMA_{0.2}) block is constant while the length of the thermo-responsive P(nPA_{0.8-co}-EA_{0.2}) block is varied. Therefore, the degree of protonation for the P(nPA_{0.8-co}-DEAEMA_{0.2}) block is expected to be the same for both P1 and P2 in the solutions.

Fig. 2 shows the transmittance curves of dilute (0.05 mg/mL) aqueous solutions of P1 and P2 upon heating at pH 7 and 10. When observed at 500 nm, a reduction in transmittance starting at ~29 °C is observed for the solutions of both P1 and P2 at pH 7 (Figs. 2A and 2B). This transition corresponds to the cloud point of the more hydrophobic second block (CP1) at pH 7, poly(nPA_{29-co}-EA₇) for P1 and poly(nPA_{70-co}-EA₁₈) for P2; the longer block has a slightly lower CP1 (Table 2), obviously an effect of the molar mass of the block. At pH 7, the poly(nPA_{28-co}-DEAEMA₇) block is partially protonated and thus more hydrophilic, but a clear

transition in transmittance (CP2) can be observed corresponding to its collapse which results in the aggregation of the particles. This transition starts at 51 °C for P1 (Fig. 2A) and 49 °C for P2 (Fig. 2B), showing that the longer hydrophobic block of P2 has a somewhat stronger effect on the collapse of the partially protonated first block at pH 7. The second transition of P1 with block ratio of 1 : 0.83 (Table 1) is close to the value reported earlier for the diblock random copolymer with the same monomer composition and similar block ratio, 1 : 1.25 (52 °C, P3 in Table 2).

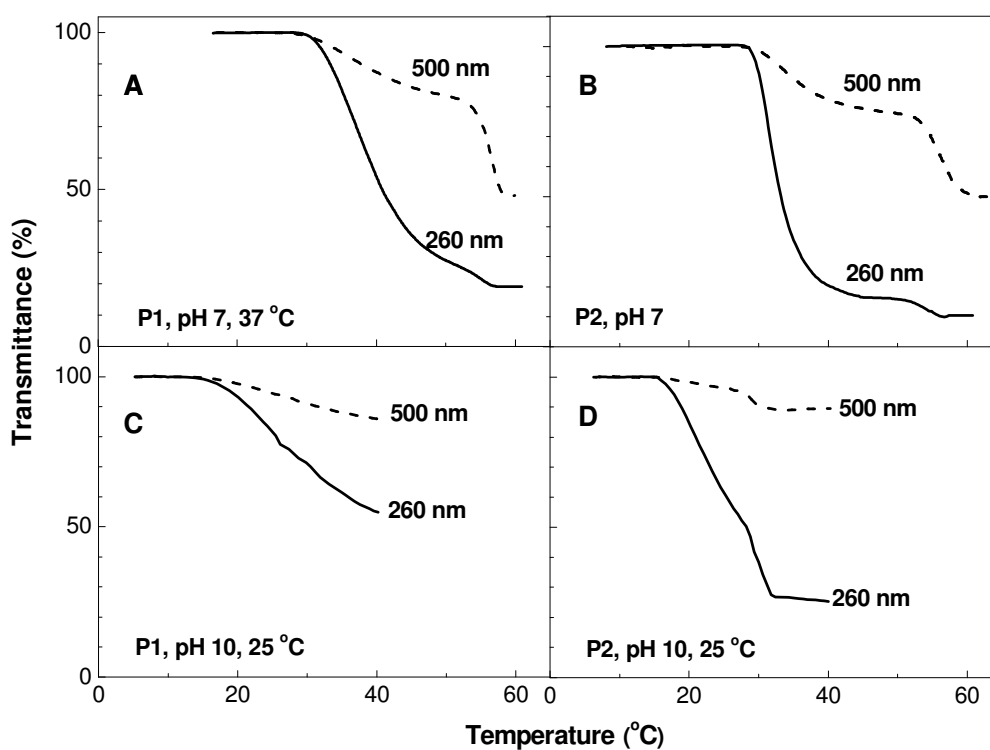


Fig. 2. Dual stimuli-responsive behavior observed for 0.05 mg/mL aqueous solutions of (A) P1 at pH 7, (B) P2 at pH 7, (C) P1 at pH 10, and (D) P2 at pH 10 measured by UV-vis transmittance at 2 different wavelengths at a heating rate of 0.3 °C/min. A two-step transition is observed in most of the curves.

At pH 10, the onset of the first transition (CP1) is observed at 14 °C, as shown in Figs. 2C and 2D for both P1 and P2. The poly(nPA₂₈-co-DEAEMA₇) block is now in its deprotonated form, making it the more hydrophobic block with a lower cloud point. The shifts in transmittance

at pH 10 are less pronounced than at pH 7, making the determination of the exact middle points of the transitions and the onset temperature of CP2 for P2 more difficult. The relatively short poly(nPA_{29-co}-EA₇) block in P1 does not show a clear change in the transmittance to yield a CP2 (Fig. 2C), while the transition for longer poly(nPA_{70-co}-EA₁₈) in P2 with a block ratio 1:2.25 starts at ~28 °C (Fig. 2D). However, a marked increase of the D_h for both P1 and P2 was observed at CP1 and CP2 in the DLS measurements at pH 10 (Fig. 3B) similar to the observation by Weiss et al.¹⁵ The strong wavelength dependence of scattering ($\sim \lambda^{-4}$) is responsible for the larger change in transmittance at a shorter wavelength (260 nm) in all the graphs of Fig. 2. All these thermally-induced transitions are reversible, and clear aggregate-free solutions were obtained by cooling the solutions below the first cloud points.

Table 2. The cloud points of the diblock random copolymers. Values measured by UV-vis transmittance at 500 nm.

		CP1 (°C) ^a		CP2 (°C) ^a		M _n (g/mol) ^b	
		Onset	Middle	Onset	Middle	1 st block	2 nd block
pH 7	P1	29	38	51	56	4,000	4,800
	P2	28	32	49	55	12,100	4,800
	P3 ^c	33	40	53	55	8,100	6,500
pH 10	P1	14	25	-	-	4,800	4,000
	P2	14	21	28	30	4,800	12,100
	P3 ^c	16	18	23	31	6,500	8,100

^aThe two values correspond to the 50% decrease in transmittance between the onset and the offset of the transmittance curves observed at 500 nm. ^bHere, the 1st and 2nd blocks under the M_n column correspond to the 1st and 2nd blocks in the sequence to aggregate, showing CP1 and CP2 at each pH, respectively. For example, the 1st block at pH 7 and 10 refers to P(nPA_{0.8-co}-EA_{0.2}) and P(nPA_{0.8-co}-DEAEMA_{0.2}), respectively. ^cP3; poly(nPA_{48-co}-DEAEMA₁₂)-block-(nPA_{43-co}-EA₁₁) prepared in our previous work.²⁸

Self-assembly of diblock random copolymers. The evolution of the mean hydrodynamic diameter (D_h) of the polymers in water at a concentration of 0.05 mg/mL was followed as a function of temperature at pH 7 and 10, and the results are shown in Fig. 3. The pH- and temperature-dependent self-assembly of block random copolymers was also visualized by TEM and AFM of freeze-dried solutions. At pH 7 and below 27 °C, the solutions consist mostly of molecularly dissolved polymer chains (Fig. 3A). However, the size distributions for both P1 and

P2 were bimodal (Figs. S1A and B†) due to the presence of a small fraction of loose aggregates arising from the interaction between the hydrophobic moieties,³⁴ which are in a fast exchange equilibrium with single chains.³⁵ The polymer chains start to self-assemble with rising temperature, and the more hydrophobic poly(nPA_{29-co}-EA₇) block in P1 and poly(nPA_{70-co}-EA₁₈) in P2 undergo a phase transition. Observed by DLS, above the first cloud point of P1, the size of the aggregates remains at ~170 nm up to 54 °C (range I in Fig. 3A). This size is larger than the contour length of the polymer would suggest for a normal radius of simple micelles or star-like aggregates (13.3 nm, Table 1). TEM (Fig. 4A) and AFM (Fig. 5A) images of a freeze-dried sample of P1 at pH 7 and 37 °C (Table 3) reveal the vesicular morphology and spherical shape of the aggregates, where the membrane inner layer should consist of the more hydrophobic P(nPA_{0.8-co}-EA_{0.2}) block. The cryo-TEM image (Figure S2A†) also shows transparent interior, indicating the hollow cavity of the vesicles. Raising the temperature above 52 °C induces an increase in D_h to ~230 nm (stage II) corresponding to another step of thermoresponsive aggregation.

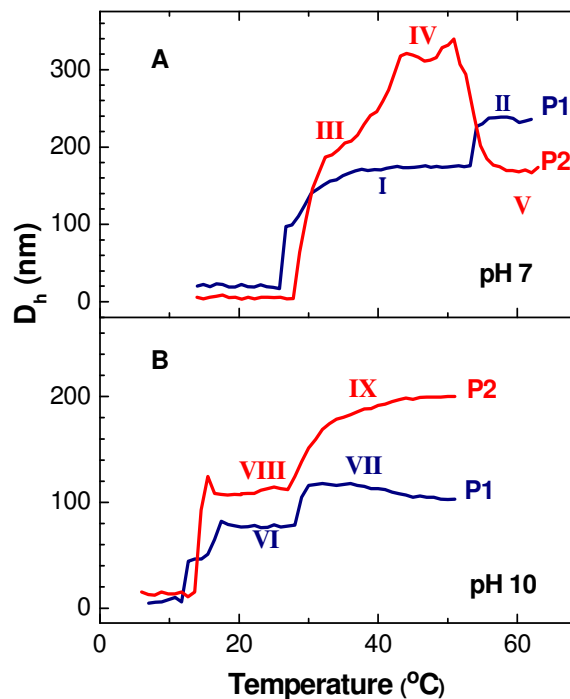


Fig. 3. Temperature dependence of the mean hydrodynamic diameter (D_h) obtained by dynamic light scattering for 0.05 mg/mL aqueous solution of P1 and P2 at (A) pH 7 and (B) pH 10.

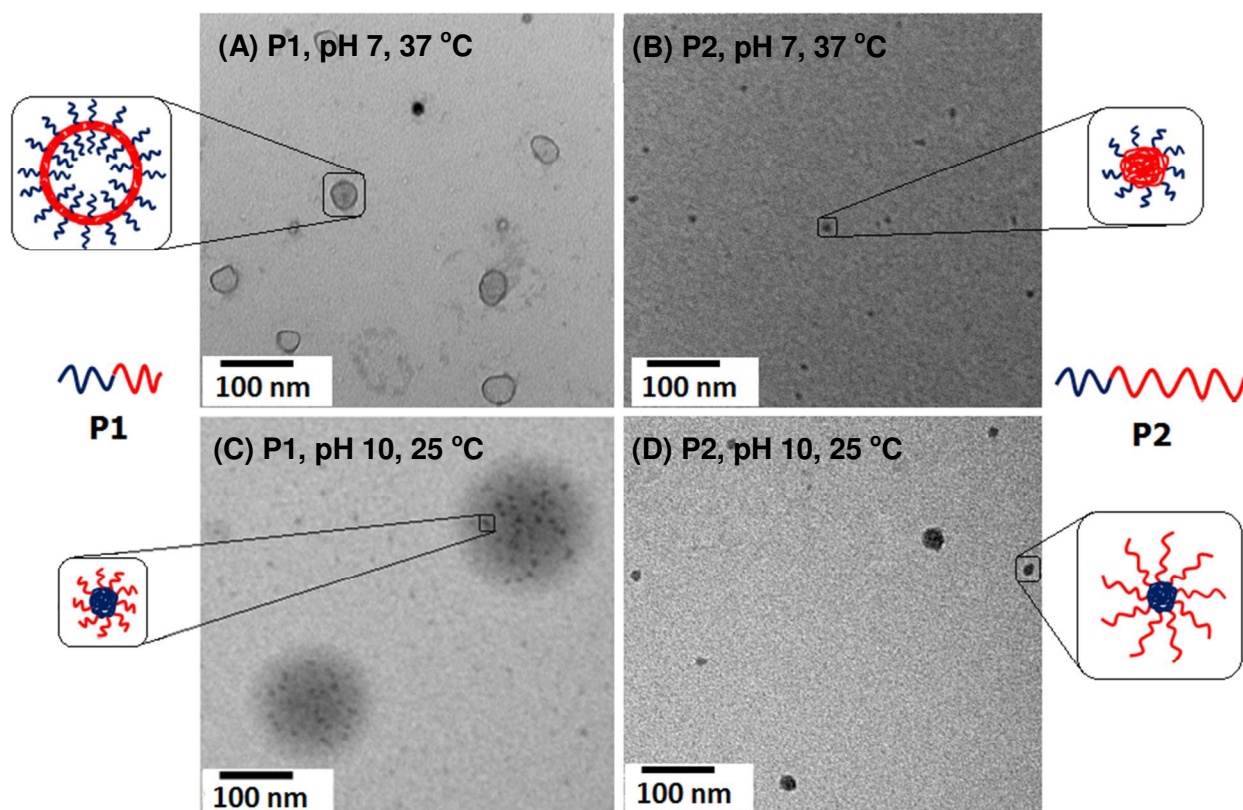


Fig. 4. TEM images of 0.05 mg/mL aqueous solutions deposited on copper grids for (A) P1 at pH 7 and 37 °C, (B) P2 at pH 7 and 37 °C, (C) P1 at pH 10 and 25 °C, and (D) P2 at pH 10 and 25 °C. The dark blue and red segments in the illustrative cartoons on the sides correspond to the poly($n\text{PA}_{0.8}\text{-}co\text{-DEAEMA}_{0.2}$) and poly($n\text{PA}_{0.8}\text{-}co\text{-EA}_{0.2}$) blocks, respectively.

Table 3. Mean diameters of self-assemblies (in nm) measured by different methods for the aqueous solutions of P1 and P2 at pH 7 and 10.

condition			CP1 < T1 < CP2			CP2 < T2		
pH	T1 (°C)	T2 (°C)	DLS ^a	AFM ^b	TEM ^b	DLS ^a	AFM ^b	
7	37	55	P1	167	75	48 (33-67)	230	138
			P2	241	65	26 (18-168)	170	125
10	25	37	P1	76	88	77 (21-212)	118	104
			P2	107	70	45 (21-442)	186	73

^aIntensity-weighted mean hydrodynamic diameter (D_h) in 0.05 mg/mL aqueous solution. ^bNumber-averaged mean diameter of dried aggregates (the size range is given in the brackets). Larger-sized aggregates are clusters of several micelles.

The behavior of P2 at pH 7 above the CP1 is quite different from that of P1. Increasing the temperature above 28 °C results in a mean hydrodynamic diameter of ~190 nm, measured by DLS (point III in Fig. 3A). Again, the size of the aggregates is larger than the contour length of P2 (20.4 nm) corresponding to the size of simple micelles (Table 1). Unlike P1, there is no evidence for vesicle formation in the TEM images of P2 (Fig. 4B). However, single micelles with collapsed poly(nPA_{70-co}-EA₁₈) core were observed by TEM (Fig. 4B) and AFM (Fig. 5B) at 37 °C. Cryo-TEM also showed dense particles with dark interior (Fig. S2B†) representing the micelles in the solution of P2 at pH 7. These micelles are swollen in their native hydrated state and bigger than the particles which may shrink in the course of freeze-drying in TEM sample preparation. Large aggregates observed by DLS were confirmed by TEM for P2 (up to 168 nm, Fig. S3A† and Table 3), indicating large clusters of micelles. The large poly(nPA_{70-co}-EA₁₈) core may not be sufficiently stabilized by the relatively short hydrophilic poly(nPA_{28-co}-DEAEMA₇) blocks, leading to the fusion of the micelles observed in cryo-TEM image (Fig. S2B†). They can even grow to clusters of the micelles with the hydrodynamic diameter of 315 nm (point IV in Fig. 3A, AFM images in Fig. S4†) at higher temperatures, similar to the observation by Weiss *et al.*¹⁵ for amphiphilic diblock copolymers. Further heating to 55 °C (Table 3) leads to the dehydration of the more hydrophilic block and the collapse of the aggregates (Figs. S5A and B†), as indicated by a decrease in D_h (stage V in Fig. 3A). The mean sizes of the aggregates estimated by the different methods for P1 and P2 below and above CP2 at pH 7 are listed in Table 3. The mean diameters obtained by AFM and TEM are the average of at least 50 particles. The charged corona of both vesicles (P1) and micelles (P2) result in the highly hydrated particles at pH 7, which lead to large hydrodynamic diameters obtained by DLS comparing to those by TEM in the dried state.

Both P1 and P2 show bimodal size distributions in the DLS measurements (Figs. S1C and D†) at pH 10 below the CP1 of the more hydrophobic block, which is now the deprotonated poly(nPA_{28-co}-DEAEMA₇). P1 shows an increase in particle size at 12 °C, while P2 shows the same increase starting at a slightly higher temperature (14 °C). This small difference may be attributed to the presence of a longer neighboring P(nPA_{0.8-co}-EA_{0.2}) block in P2 (poly(nPA_{70-co}-EA₁₈)). Both polymers show two transitions in Fig. 3B with a plateau between CP1 and CP2 (30 °C). The shorter hydrophilic block in P1 results in a smaller mean hydrodynamic diameter of the aggregates at 25 °C (76 nm, point VI in Fig. 3B) than in the case of P2 (107 nm, point VIII in

Fig. 3B). On the basis of TEM (Figs. 4C and D) and AFM (Figs. 5C and D) images, small micelles with collapsed poly($n\text{PA}_{28}\text{-}co\text{-DEAEMA}_7$) core were observed together with large aggregates of the micelles for both P1 and P2 at 25 °C (Table 3). Similar to the DLS data, in TEM images also the large aggregates of P1 (Fig. 4C) have smaller diameters than P2 (Fig. S3B†). On the other hand, the longer hydrophilic block in P2 leads to the formation of more stable micelles at pH 10. Therefore, single micelles contribute to the majority of the particles formed by P2 at pH 10 (Fig. 4D), while P1 at pH 10 mostly forms micellar clusters, which are aggregates of many micelles (Fig. 4C). Increasing the temperature to 37 °C (Table 3), above the CP2 of both P1 and P2, leads to the dehydration and collapse of the poly($n\text{PA}_{0.8}\text{-}co\text{-EA}_{0.2}$) block accompanied by further aggregation resulting in an increase in particle size corresponding to stages VII and IX in Fig. 3B for P1 and P2, respectively. This is also observed in the AFM images of the aggregates at 37 °C (Fig. S5C and D†). The mean sizes of aggregates estimated by the different methods for P1 and P2 below and above the CP2 at pH 10 are listed in Table 3. As expected, larger and less regular aggregates are obtained above the CP2 for P2 with a longer corona block, similar to the results of Laschewsky and coworkers¹⁵ for $\text{PnPA-}b\text{-PEA}$ with longer PEA block. While P2 continued to aggregate with increasing temperature, P1 shows a slight decrease in D_h upon further heating. This difference may arise from the different lengths of the corona blocks.

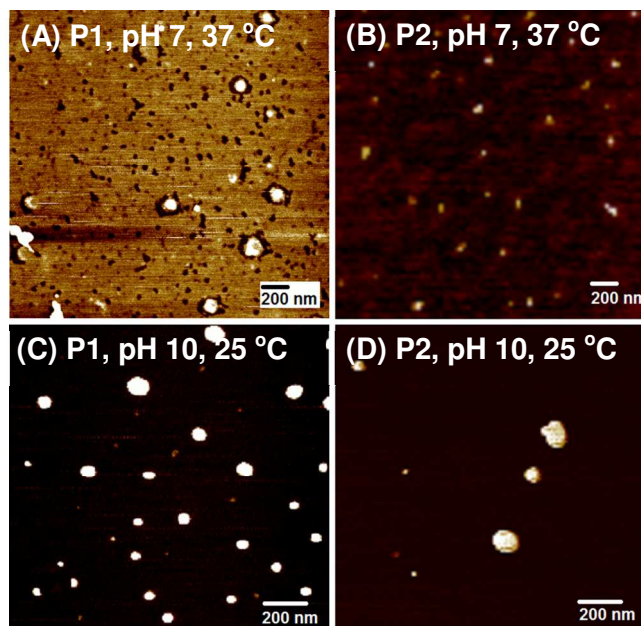
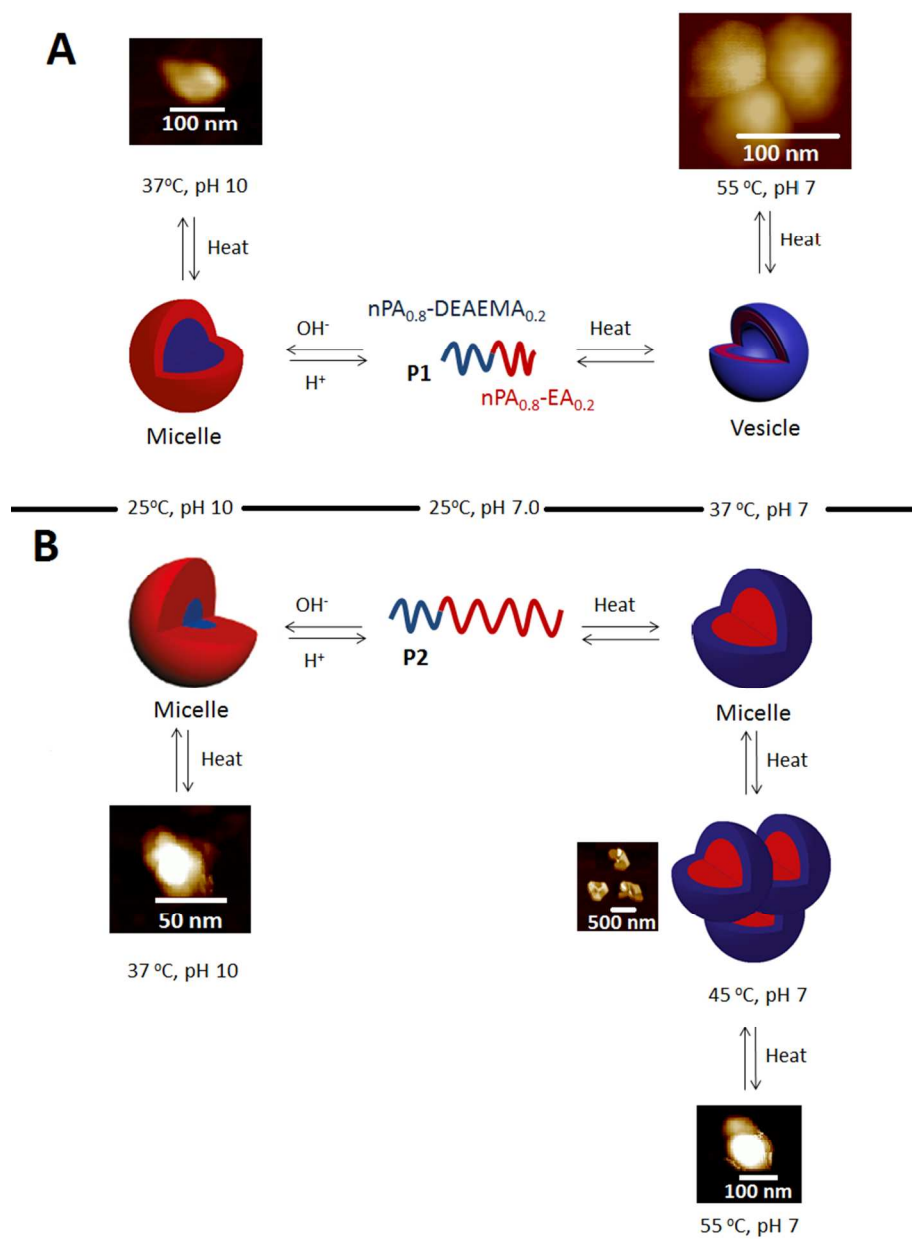


Fig. 5. AFM images of aqueous solutions (0.05 mg/mL) of P1 and P2 above their CP1, deposited on mica. (A) P1 at pH 7 and 37 °C, (B) P2 at pH 7 and 37 °C, (C) P1 at pH 10 and 25 °C, and (D) P2 at pH 10 and 25 °C.

P1 is a nearly symmetric block copolymer, where the ratio of poly($n\text{PA}_{28}\text{-}co\text{-DEAEMA}_7$) and poly($n\text{PA}_{29}\text{-}co\text{-EA}_7$) blocks is 53:47 weight percentage ratio (wt%), and with this composition, either vesicles or micelles may be formed as reported in the literature on stimuli-responsive block copolymers.^{16, 22, 26, 28} When the temperature of its solution at pH 7 is raised to 37 °C, the polymer chains self-assemble to form vesicles with the poly($n\text{PA}_{29}\text{-}co\text{-EA}_7$) and poly($n\text{PA}_{28}\text{-}co\text{-DEAEMA}_7$) blocks as the inner and outer layers of the membrane, respectively, as depicted in Scheme 1A. Heating above the CP of the poly($n\text{PA}_{28}\text{-}co\text{-DEAEMA}_7$) block leads to aggregation, and large clusters of spherical aggregates can be observed by AFM (Figs. S5A and B†). On the other hand, increasing the pH of the solution of P1 up to 10 at a constant temperature of 25 °C results in the formation of spherical micelles with a poly($n\text{PA}_{28}\text{-}co\text{-DEAEMA}_7$) core and a poly($n\text{PA}_{29}\text{-}co\text{-EA}_7$) corona, which aggregate further when the temperature rises above the CP of the poly($n\text{PA}_{29}\text{-}co\text{-EA}_7$) block. Interestingly, vesicles were obtained in our previous study²⁸ under the same conditions for P($n\text{PA}_{0.8}\text{-}co\text{-DEAEMA}_{0.2}$)-*b*-P($n\text{PA}_{0.8}\text{-}co\text{-EA}_{0.2}$) with a slightly different block ratio, 45:55 wt%, and longer blocks (6500 and 8100 g/mol vs. 4800 and 4000 g/mol of the current work). This suggests that the composition of the block random copolymer may be quite critical for the self-assembly process, and the

compositions close to 50:50 wt% could be on the threshold of different aggregate morphologies for such a polymer system.

The ratio of poly(nPA_{28-co}-DEAEMA₇) and poly(nPA_{70-co}-EA₁₈) blocks in P2 is 32:68 wt%. This polymer forms invertible micelles at pH 7 and 10 above the CP of the more hydrophobic block (CP1), where the core and the shell blocks may be switched according to the pH of the solution. Micelles at pH 7 with the shorter hydrophilic shell (protonated poly(nPA_{28-co}-DEAEMA₇)) are smaller than their inverted counterparts at pH 10 with poly(nPA_{70-co}-EA₁₈) as the hydrophilic shell (Fig. 4B and Table 3). Moreover, because of the much longer poly(nPA_{70-co}-EA₁₈) block in the core, further aggregation was observed for the micelles with poly(nPA_{28-co}-DEAEMA₇) shell, and large clusters of the aggregates are observed for P2 at pH 7 and 45 °C (Scheme 1B), which collapse when heated above the CP of the poly(nPA_{28-co}-DEAEMA₇) block (55 °C in Scheme 1B). The morphological changes of P1 and P2 are different from those observed for pH- and temperature-responsive poly(*N,N*-diethylaminoethyl methacrylate)-*block*-poly(*N*-isopropylacrylamide) (PDEAEMA-*b*-PNIPAM), which forms spherical micelles at a block ratio of 47:53 wt% at high pH or high temperature, but shows a micelle-to-vesicle transition at the composition of 29:71 wt%.¹⁶ In that case, each of the blocks responds to a different stimulus, while introducing a dually-responsive block into a thermo-responsive block brings about double thermo-sensitivity and, at the same time, makes the aggregation behavior of our system more complex, as indicated by the visually observable polydispersity and large sizes of the aggregates. Therefore, Scheme 1 represents only a simplified picture of the self-assembly of the real system.



Scheme 1. Invertible micellization behavior of (A) P1, above, and (B) P2, below, in water by changing the temperature and pH, showing the effect of block length ratios (Table 1). The representative images were taken from larger AFM images.

Conclusion

Dually-responsive diblock random copolymers are capable of forming either micells or vesicles in aqueous solutions. The change in the relative hydrophilicity of the blocks results in

inverted structures, and may switch the self-assembled morphology between vesicles and micelles. In general, molecularly dissolved polymer chains together with loose aggregates co-exist at a lower temperature, but larger aggregates form above the cloud point of the copolymer. In the case of the symmetric diblock copolymer P1 of similar block lengths, vesicles may form during heating, while micelles are obtained together with micellar aggregates by raising the pH. The process is accompanied by a switch of the more hydrophobic block of the copolymer. Upon changing the relative lengths of the blocks as in the case of P2 with a much longer second block, micelles with a small fraction of micellar aggregates form under identical conditions while the core and shell of the micelles switch when the stimuli (temperature or pH changes) are applied. The charged shell and repulsive forces are responsible for the stability of the micelles at pH 7, while the micelles at pH 10 are stable due to the long hydrophilic corona. The ease in the adjustment of the composition and block length in the preparation of such copolymers provides the possibility of making a variety of copolymers which may form different types of aggregates in aqueous solutions and may switch or change their assembled structures under controllable conditions. Switching between vesicles and micelles may provide a convenient way for fast release of encapsulated reagents. The positively-charged surface of the vesicles in the case of the protonated form of the polymer may interact with biological membranes via electrostatic interactions destined for biochemical applications.

Acknowledgments

Financial support from NSERC of Canada, the FQRNT of Quebec, and the Canada Research Chair program is gratefully acknowledged. The authors are members of CSACS funded by FQRNT and GRSTB funded by FRSQ.

† Electronic supplementary information (ESI) available: AFM images of the P2 between CP1 and CP2, point IV in Fig. 3A, and AFM images of P1 and P2 above their CP2 at pH 7 and 10.

References

1. O. Borisov, E. Zhulina, F. M. Leermakers and A. E. Müller, in *Self Organized Nanostructures of Amphiphilic Block Copolymers I*, eds. A. H. E. Müller and O. Borisov, Springer Berlin Heidelberg, 2011, vol. 241, pp. 57-129.

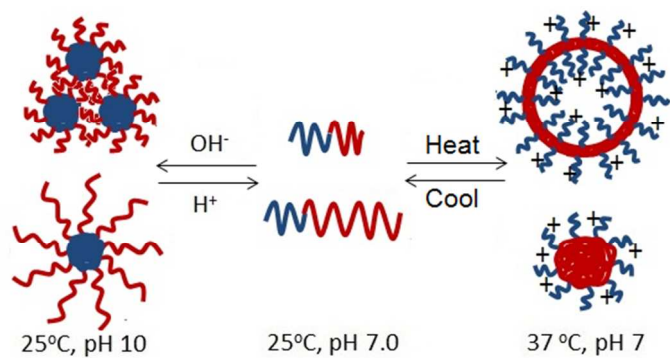
2. H. Cui, Z. Chen, S. Zhong, K. L. Wooley and D. J. Pochan, *Science*, 2007, **317**, 647-650.
3. G. Riess, *Prog. Polym. Sci.*, 2003, **28**, 1107-1170.
4. J. A. Opsteen, J. J. L. M. Cornelissen and J. C. M. v. Hest, *Pure Appl. Chem.*, 2004, **76**, 1309-1319.
5. J.-F. Gohy, in *Block Copolymers II*, ed. V. Abetz, Springer Berlin Heidelberg, 2005, vol. 190, pp. 65-136.
6. S. J. Holder and N. A. J. M. Sommerdijk, *Polym. Chem.*, 2011, **2**, 1018-1028.
7. J. Du and R. K. O'Reilly, *Soft Matter*, 2009, **5**, 3544-3561.
8. S. Förster, V. Abetz and A. E. Müller, in *Polyelectrolytes with Defined Molecular Architecture II*, ed. M. Schmidt, Springer Berlin Heidelberg, 2004, vol. 166, pp. 173-210.
9. D. E. Discher and A. Eisenberg, *Science*, 2002, **297**, 967-973.
10. V. Bütün, N. C. Billingham and S. P. Armes, *J. Am. Chem. Soc.*, 1998, **120**, 11818-11819.
11. F. A. Plamper, J. R. McKee, A. Laukkanen, A. Nykanen, A. Walther, J. Ruokolainen, V. Aseyev and H. Tenhu, *Soft Matter*, 2009, **5**, 1812-1821.
12. S. Liu, N. C. Billingham and S. P. Armes, *Angew. Chem. Int. Ed.*, 2001, **40**, 2328-2331.
13. Y.-J. Shih, Y. Chang, A. Deratani and D. Quemener, *Biomacromolecules*, 2012, **13**, 2849-2858.
14. D. Xie, X. Ye, Y. Ding, G. Zhang, N. Zhao, K. Wu, Y. Cao and X. X. Zhu, *Macromolecules*, 2009, **42**, 2715-2720.
15. J. Weiss, C. Böttcher and A. Laschewsky, *Soft Matter*, 2011, **7**, 483.
16. A. E. Smith, X. Xu, S. E. Kirkland-York, D. A. Savin and C. L. McCormick, *Macromolecules*, 2010, **43**, 1210-1217.
17. E. S. Read and S. P. Armes, *Chem. Commun.*, 2007, 3021-3035.
18. I. K. Voets, A. de Keizer, P. de Waard, P. M. Frederik, P. H. H. Bomans, H. Schmalz, A. Walther, S. M. King, F. A. M. Leermakers and M. A. Cohen Stuart, *Angew. Chem. Int. Ed.*, 2006, **45**, 6673-6676.
19. S. Venkataraman, A. L. Lee, H. T. Maune, J. L. Hedrick, V. M. Prabhu and Y. Y. Yang, *Macromolecules*, 2013, **46**, 4839-4846.
20. W. F. Edmonds, Z. Li, M. A. Hillmyer and T. P. Lodge, *Macromolecules*, 2006, **39**, 4526-4530.
21. X. Wang, G. Guerin, H. Wang, Y. Wang, I. Manners and M. A. Winnik, *Science*, 2007, **317**, 644-647.
22. C. Pietsch, U. Mansfeld, C. Guerrero-Sanchez, S. Hoepfner, A. Vollrath, M. Wagner, R. Hoogenboom, S. Saubern, S. H. Thang, C. R. Becer, J. Chiefari and U. S. Schubert, *Macromolecules*, 2012, **45**, 9292-9302.
23. L. Luo and A. Eisenberg, *J. Am. Chem. Soc.*, 2001, **123**, 1012-1013.
24. K. Yu and A. Eisenberg, *Macromolecules*, 1998, **31**, 3509-3518.
25. Y. Chen, J. Du, M. Xiong, H. Guo, H. Jinnai and T. Kaneko, *Macromolecules*, 2007, **40**, 4389-4392.
26. M. T. Savoji, S. Strandman and X. X. Zhu, *Macromolecules*, 2012, **45**, 2001-2006.
27. Y. Kotsuchibashi, M. Ebara, N. Idota, R. Narain and T. Aoyagi, *Polym. Chem.*, 2012, **3**, 1150.

28. M. T. Savoji, S. Strandman and X. X. Zhu, *Langmuir*, 2013, **29**, 6823-6832.
29. D. M. Vriezema, M. Comellas Aragonès, J. A. A. W. Elemans, J. J. L. M. Cornelissen, A. E. Rowan and R. J. M. Nolte, *Chem. Rev.*, 2005, **105**, 1445-1490.
30. K. J. Shea, G. J. Stoddard, D. M. Shavelle, F. Wakui and R. M. Choate, *Macromolecules*, 1990, **23**, 4497-4507.
31. M. H. Stenzel, T. P. Davis and A. G. Fane, *J. Mater. Chem.*, 2003, **13**.
32. J.-S. Park and K. Kataoka, *Macromolecules*, 2007, **40**, 3599-3609.
33. P. Xiang and Z. Ye, *J. Polym. Sci., Part A: Polym. Chem.*, 2013, **51**, 672-686.
34. M. Nichifor, A. Lopes, A. Carpov and E. Melo, *Macromolecules*, 1999, **32**, 7078-7085.
35. J. Yan, W. Ji, E. Chen, Z. Li and D. Liang, *Macromolecules*, 2008, **41**, 4908-4913.

Table of Contents only

Invertible vesicles and micelles formed by dually-responsive diblock random copolymers in aqueous solutions

Mohammad T. Savoji, Satu Strandman, X.X. Zhu*



Or

